Journal of Inorganic Biochemistry 223 (2021) 111524

Contents lists available at ScienceDirect

Journal of Inorganic Biochemistry

journal homepage: www.elsevier.com/locate/jinorgbio

Synthesis, characterization and catalytic activity of a mononuclear nonheme copper(II)-iodosylbenzene adduct

Hyeri Jeon, Hana Oh, Seungwoo Hong *

Department of Chemistry, Sookmyung Women's University, 04310, Seoul, 03722, Republic of Korea

ARTICLE INFO

Keywords:
Reactive intermediate
Iodosylbenzene adduct
Intramolecular H-bonding
Electron transfer
Catalytic reaction Cu(II) complex

ABSTRACT

Iodosylbenzene (PhIO) and its derivatives have attracted significant attention due to their various applications in organic synthesis and biomimetic studies. For example, PhIO has been extensively used for generating high-valent metal-oxo species that have been regarded as key intermediates in diverse oxidative reactions in biological system. However, recent studies have shown that metal-iodosylbenzene adduct, known as a precursor of metal-oxo species, plays an important role in transition metal-catalyzed oxidation reactions. During last few decades, extensive investigations have been conducted on the synthesis and reactivity studies of metal-iodosylbenzene adducts with early and middle transition metals including manganese, iron, cobalt. Nevertheless, metal-iodosylbenzene adducts with late transition metals such as nickel, copper and zinc, still remains elusive. Herein, we report a novel copper(II)-iodosylbenzene adduct bearing a linear ligand composed of two pyridine rings and an ethoxyethanol side-chain, $[Cu(OIPh)(HN_3O_2)]^{2+}$ (**1**). The copper(II)-iodosylbenzene adduct was characterized by several spectroscopic methods including UV–vis spectroscopy, electrospray ionization mass spectrometer (ESI MS), and electron paramagnetic resonance (EPR) combined with theoretical calculations. Interestingly, **1** can carry out the catalytic sulfoxidation reaction. In sulfoxidation reaction with thioanisole under catalytic reaction condition, not only two-electron but also four-electron oxidized products such sulfoxide and sulfone were yielded, respectively. However, **1** was not an efficient oxidant towards C—H bond activation and epoxidation reactions due to the steric hindrance created by the intramolecular H-bonding interaction between HN_3O_2 ligand and iodosylbenzene moiety.

1. Introduction

Copper containing metalloenzymes conducts reductive activation of dioxygen mediated fundamental processes, which govern a myriad of biological functions such as cellular respiration and oxidative transformation of biomolecules [1–10]. Tremendous efforts towards understanding how these oxidation and oxygenation processes occur have led many researchers to pinpoint spectroscopic features of plausible copper oxygen intermediates, disclose their reactivity and provide detailed mechanistic information [11–16]. Among proposed copper oxygen intermediates, less is known about high-valent mononuclear copper-oxo $[CuO]^+$ species, namely Cu(III)-oxo or Cu(II)-oxyl radical complexes due to their intrinsic instability; only theoretical and gas-phase investigations predict their existence and their particularly high reactivity, thereby, great controversy and debate persisted over pros and cons of their formation [17–22].

Remarkable oxidizing properties of hypervalent iodine(III) and (IV) reagents have led to an increased interest in rapid development in the syntheses and functionalization of heterocyclic compounds via facilitating atom transfer reactions [23]. While iodosylbenzene (PhIO) has been tremendously used as an oxygen atom source in transition metal-catalyzed functionalization of hydrocarbons, great efforts have been devoted to uncover the mechanistic insights into high-valent metal-oxo species and their reactivity patterns by promoting "shunt pathway" with aliquots of PhIO. Multiple examples of heme and nonheme metal-oxo species, which were central in catalytic properties of various interfaces have been synthesized and spectroscopically characterized [24–30]. Therefore, one of solid consensus approach of generating the metal-oxo, $[MO]^{2+}$, is by reacting various model complexes with PhIO.

More recently, accumulated evidences that come under recent scrutiny supported that the iodosylbenzene adducts of metal complexes, [M-OIPh], were successfully prepared, isolated and characterized spectroscopically despite that their generation was transient and unstable [31]. For example, the structure and reactivity of an iodosylarene adduct

* Corresponding author.
E-mail address: hsw@sookmyung.ac.kr (S. Hong).

https://doi.org/10.1016/j.jinorgbio.2021.111524
Received 30 April 2021; Received in revised form 11 June 2021; Accepted 25 June 2021
Available online 29 June 2021

of heme and nonheme Mn(III), Mn(IV), and Fe(III) complexes have been extensively investigated [32–38]. On the basis of this discovery, multiple-oxidant mechanism, in which metal-iodosylarene adducts were proposed as a precursor of high-valent metal-oxo intermediates, was surged and some of them exhibited the reactivity superior to their corresponding metal-oxo intermediates. Moving from iron to late transition metals such as cobalt, nickel, and copper, the formation of high-valent metal-oxo species is theoretically inaccessible in tetragonal geometry by virtue of the "oxo wall" coined by Gray and Ballhausen [22,39]. It predicts eventual electron population in an M–O π* antibonding orbital resulting in the decrease of the bond order below 2. Instead, the formation of iodosylarene adduct of cobalt(II) and cobalt(III) complexes were evidenced crystallographically [40,41]. However, the iodosylarene adduct of copper complexes still remained rare to date. Herein, we report the synthesis and spectroscopic characterization of a copper(II) iodosylbenzene adduct, $[Cu(OIPh)(HN_3O_2)]^{2+}$ (**1**; HN_3O_2 = 2-(2-(bis(pyridin-2-ylmethyl)amino)ethoxy)ethanol) (Scheme 1). DFT optimized structures suggest that H-bonding interaction can be formed to the proximal oxygen atom in iodosylbenzene moiety in order to afford an additional thermal stability. We then investigate its redox and electron-transfer properties and examine the kinetic behaviors in catalytic reactions such as C—H bond activation, oxygen atom transfer and olefin epoxidation reactions. Although slow reactivity was confirmed, **1** shows moderate catalytic oxygen atom transfer reactivity, however, sluggish reactivity in the C—H bond activation, and olefin epoxidation reactions.

2. Experiments

2.1. Materials

All chemicals were obtained from Aldrich Chemical Co. and used without further purification unless otherwise indicated. Solvents were dried according to the reported procedures and distilled under Ar prior to use [42]. $H_2^{18}O$ (95% ^{18}O-enriched) was purchased from ICON Services Inc. (Summit, NJ, USA). The mononuclear nonheme copper(II) complex, $[Cu(HN_3O_2)(CH_3CN)(H_2O)](ClO_4)_2$, was prepared according to the literature methods [43].

Caution! *The peroxidized compound and perchlorate ion should be treated as potential bombs. This can be done safely for relatively low levels of peroxides and perchlorate ions (2 mM and 2.0 mL volume).*

2.2. Instrumentation

UV−vis spectra were recorded on a Hewlett-Packard Agilent 8453 UV−visible spectrophotometer equipped with a T2/sport temperature controlled cuvette holder. Electrospray ionization mass spectra (ESI MS) were collected on a Thermo Finnigan (San Jose, CA, USA) LTQ XL ion trap instrument, by infusing samples directly into the source at 5.0 μL/min using a syringe pump. The spray voltage was set at 4.7 kV and the capillary temperature at 200 °*C. electron* paramagnetic resonance (EPR) spectra were recorded at 80 K using an X-band Bruker EMX-plus spectrometer equipped with a dual mode cavity (ER 4116DM). The low temperatures were achieved and controlled by an Oxford Instruments ESR900 liquid He quartz cryostat with an Oxford Instruments ITC503 temperature and gas flow controller. The experimental parameters for EPR measurements were as follows: microwave frequency = 9.646 GHz, microwave power = 1.0 mW, modulation amplitude = 10 G, gain = 1 × 104, modulation frequency = 100 kHz, time constant = 40.96 ms, and conversion time = 85.00 ms. Product analyses were performed with an Agilent 1220 infinity II high performance liquid chromatograph (HPLC), and Agilent Technologies 6890 N gas chromatograph (GC). Electrochemical measurements were performed on a CHI630B electrochemical analyzer (CH Instruments, Inc.) in CH_3CN containing 0.10 M Bu_4NPF_6 ($TBAPF_6$) as a supporting electrolyte at 293 K. A conventional three-electrode cell was used with a platinum working electrode (surface area of 0.30 mm^2), a platinum wire as a counter electrode, and a Ag/Ag^+ electrode as a reference electrode. The platinum working electrode was routinely polished with BAS polishing alumina suspension and rinsed with acetone and acetonitrile before use. The measured potentials were recorded with respect to a Ag/Ag^+ (0.010 M) reference electrode.

2.3. Generation and characterization of $[Cu(OIPh)(HN_3O_2)]^{2+}$ (1)

The mononuclear nonheme copper(II) iodosylbenzene adduct, $[Cu(OIPh)(HN_3O_2)]^{2+}$ (**1**), was prepared by treating a CH_3CN-solution of $[Cu(HN_3O_2)(CH_3CN)(H_2O)](ClO_4)_2$ with 3.0 equiv. of PhIO in CH_3CN at 293 K. The formation of **1** was confirmed by monitoring the band growth at 345 nm from UV−vis spectral changes of the reaction solution. The electron paramagnetic resonance (EPR) spectra of **1** (1.0 mM) were recorded at 4 K. ^{18}O-labeled sample of **1**, $[Cu(^{18}OIPh)(HN_3O_2)]^{2+}$ (**1-^{18}O**), was prepared by using ^{18}O-labeled PhIO, which was synthesized by incubating PhIO in MeOH (5% $H_2^{18}O$).

2.4. Kinetic studies and product analysis

All reactions were run in 1 cm UV quartz cuvette and followed by monitoring UV−vis spectral changes of reaction solutions. Rate constants were determined under pseudo-first-order conditions (e.g., [substrate]/[**1**] > 10) by fitting the changes in absorbance for the disappearance of bands at 345 nm for **1**, 620 nm for ferrocene, and 650 nm for dimethylferrocene, respectively, in the phosphorus oxidation and electron transfer reactions. The catalytic reactions of **1** with thioanisole, cyclohexene, and styrene were conducted in CH_3CN at 293 K. The kinetic experiments were run at least in triplicate, and the data reported represent the average of these reactions.

Organic products formed in the catalytic reactions of **1** with thioanisole, cyclohexene and styrene were analyzed by high performance liquid chromatography (HPLC) and gas chromatography (GC). The product yields were determined by comparing the peak areas of sample

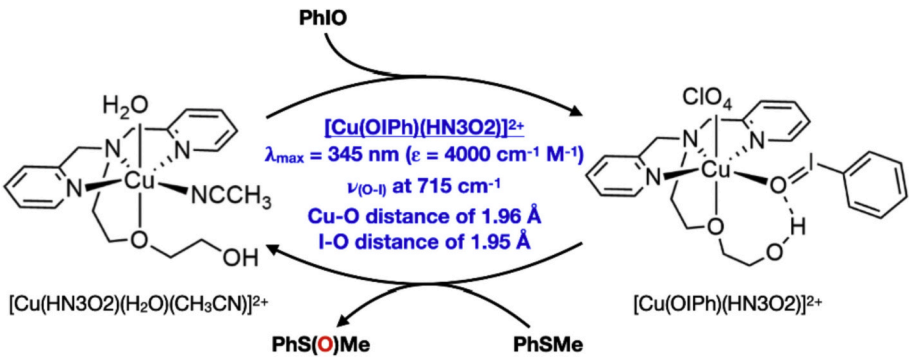

Scheme 1. Schematic representation showing synthesis, characterization and reactivity of $[Cu(OIPh)(HN_3O_2)]^{2+}$.

products against standard curves prepared with known authentic samples.

2.5. Density functional theory calculations

Geometry optimizations of **1a**, and **1b** were directly modified from the single-crystal structure of $[Cu^{II}(HN_3O_2)(CH_3CN)(H_2O)](ClO_4)_2$. In **1b**, the intramolecular H-bond interactions between the H atom of the HN_3O_2 ligand and the O atom of iodosylbenzene was included. All structures were fully optimized by using the Gaussian 09 [44] program with the B3LYP density functional at the LANL2DZ/6-31G** level [45–58], whereas no imaginary frequencies were observed. In addition, the solvent effect of the polarizable continuum model (PCM) with acetonitrile ($\varepsilon = 35.688$) and temperature (293 K) was also applied [59]. Energy evaluation were done at B3LYP/LANL2DZ/6–311 + G** level [45–48,60–69] on the structure obtained by B3LYP/LANL2DZ/6-31G**.

3. Results and discussion

3.1. Synthesis and characterization of iodosylbenzene adduct copper(II) complex

The copper(II) complex coordinated with a HN_3O_2 ligand, $[Cu(HN_3O_2)(CH_3CN)(H_2O)](ClO_4)_2$, was synthesized according to the literature methods [43]. Addition of iodosylbenzene (PhIO) into a CH_3CN-solution containing $[Cu(HN_3O_2)(CH_3CN)(H_2O)](ClO_4)_2$ afforded gradual solution colour change from blue to pale blue along with appearance of absorption band at 345 nm ($\varepsilon = 2200\ cm^{-1}\ M^{-1}$) and at 641 nm ($\varepsilon = 100\ cm^{-1}\ M^{-1}$) 293 K (Fig. 1a). According to the spectroscopic titration, the absorbance at 345 nm due to **1** was saturated when 3.0 equiv. of PhIO was added (Fig. S1). The colour of resulting solution of this new species, denoted as **1**, was metastable with a half-life time ($t_{1/2}$) of ~30 min allowing us to spectroscopically characterize **1**. It is noteworthy that the stability of other metal-iodosylbenzene adducts in a tetragonal geometry were markedly increased in a mixture solvent system (e.g, acetone:trifluoroethanol) or in the presence of acids (e.g., perchloric acid) [36–38,41]. However, the addition of perchloric acid resulted in the fast decay of **1**. To verify the formation of iodosylbenzene adduct of copper complex, electrospray ionization mass (ESI MS), electron paramagnetic resonance (EPR), and infrared (IR) spectroscopic measurements were conducted. The ESI MS spectrum of **1** exhibited minor mass peaks at *m/z* of 668.5, whose mass and isotope distribution patterns were fully consistent with $[Cu(OIPh)(HN_3O_2)(ClO_4)]^+$ (calculated *m/z* of 668.9) (Fig. 1b). When **1** was synthesized with ^{18}O isotope labeling PhIO ($PhI^{18}O$), a two mass unit shift from *m/z* of 668.5 to 670.5 was observed, suggesting the incorporation of an oxygen atom within **1** (Fig. 1b, inset). The IR spectrum of **1** showed isotopically sensitive infrared bands at 715 cm^{-1}, which was shifted to 678 cm^{-1} upon the use of $PhI^{18}O$ (Fig. 1c). The observed shift of $\Delta = 37\ cm^{-1}$ was in a good agreement with the calculated value of 36 cm^{-1} expected for a diatomic O—I oscillator dictated by Hooke's law. Compared to the O—I bond stretching frequencies of other reported metal-iodosylbenzene adduct that appeared in the range of 600–750 cm^{-1} [32–38,40,41], **1** showed relatively strong O—I bond vibrational energy due to low oxidation state of copper. The EPR spectrum of **1**, recorded in a frozen CH_3CN solution at 4 K, exhibited a rhombic signal at $g = 2.28$ ($A = 120$ G), 2.05 and 1.98 (Fig. S2). Such moderate hyperfine coupling constant value (A) of **1** implied that the geometry of **1** is slightly distorted square planar, thereby, a distorted tetragonally elongated geometry of **1** due to Jahn-Teller disortion was anticipated.

3.2. Density functional theory (DFT) calculations

To gain insight into structural information, DFT calculations was performed on the iodosylbenzene adduct of copper(II) complex, **1**. Given that HN_3O_2 ligand was prone to form the intramolecular H-bonding

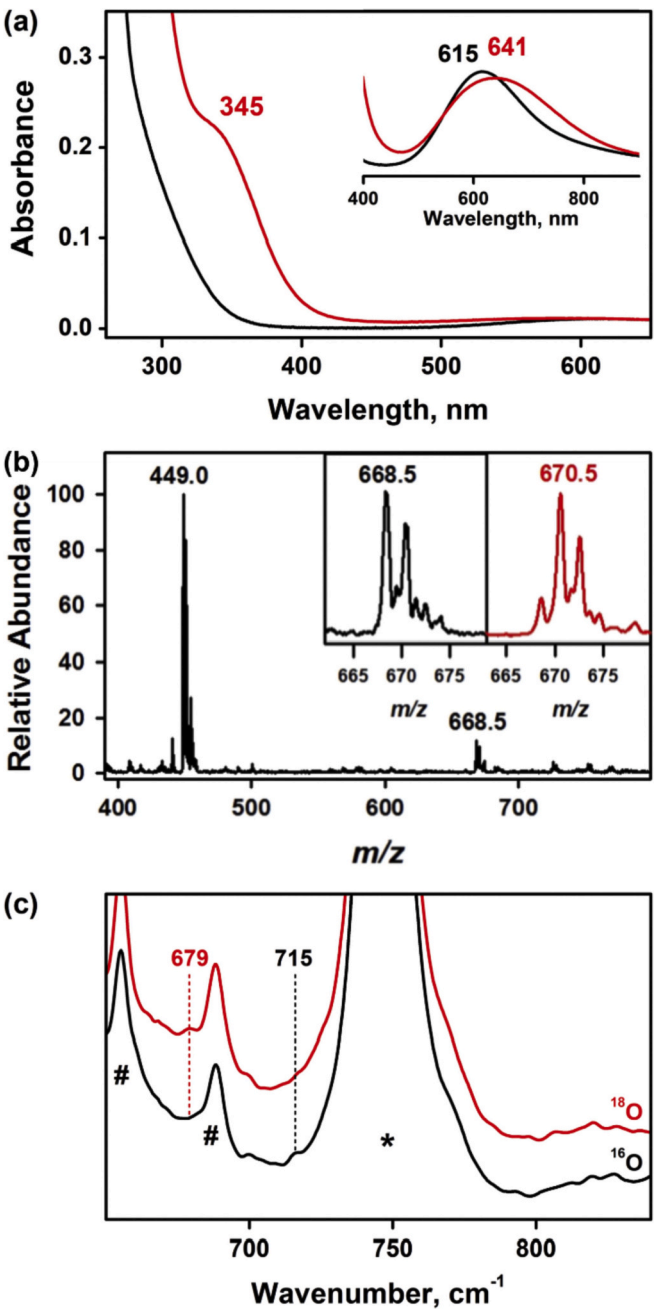

Fig. 1. (a) UV–vis spectra obtained in the reaction of **1** (0.10 mM) with iodosylbenzene (0.30 mM) in CH_3CN at 293 K. Inset shows the visible spectrum of **1** (2.0 mM) in the region of 400–900 nm. (b) ESI MS spectra of **1** (0.10 mM) and ^{18}O-labeled **1**. The peaks at *m/z* of 449.0 and 668.5 correspond to $[Cu(HN_3O_2)(ClO_4)]^+$ (calculated *m/z* of 449.1) and $[Cu(OIPh)(HN_3O_2)(ClO_4)]^+$ (calculated *m/z* of 668.9), respectively. Insets show the observed isotope distribution patterns of **1** and ^{18}O-labeled **1**. (c) IR spectra of solid **1** (black line) and ^{18}O-labeled **1** (red line). * and # are indicative of solvent and ligand peaks, respectively. (For interpretation of the references to colour in this figure legend, the reader is referred to the web version of this article.)

interaction, we first constructed two possible structures of **1** with and without H-bonding from the known crystal structure of $[Cu(HN_3O_2)(CH_3CN)(H_2O)]^{2+}$, **1a** and **1b**, respectively and carried out their structural optimization [43]. DFT optimized structures of both **1a** and **1b** are shown in Fig. 2. For **1a** without intramolecular H-bonding, the optimized structure of the ground state showed tetragonally elongated geometry around the Cu center with a Cu—O distance of 1.942 Å (Fig. 2, left). This bond distance was in line with other structurally characterized

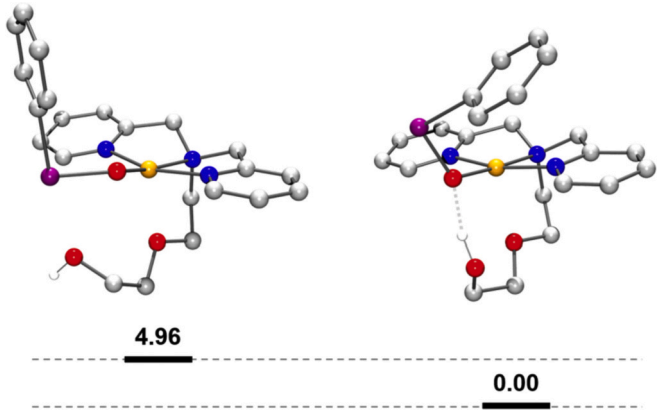

Fig. 2. DFT optimized structures of **1** without (left) and with H-bonding interaction (right) between HN_3O_2 ligand and iodosylbenzene moiety. Colors for the structures: Cu, orange; N, blue; O, red; I, purple; C, pale gray; H, white. Relative energy diagram (bottom) of **1a** and **1b**. (For interpretation of the references to colour in this figure legend, the reader is referred to the web version of this article.)

iodosylbenzene adduct of metal complexes [32–38,40,41]. In case of **1b** with intramolecular H-bonding, the Cu—O distance was slightly elongated to 1.958 Å due to the weakening of the Cu—O bond in comparison to the structure of **1a** without H-bonding at oxygen atom (Fig. 2, right). The relative energies of **1a** and **1b** were illustrated in Fig. 2. The relative energies diagram showed that **1a** was energetically unfavorable than **1b**; the energy of **1b** is lower (ca. 4.96 kcal/mol) than that of **1a**; this clearly suggested that the H-bonding interaction between the HN_3O_2 ligand and the proximal oxygen atom of the iodosylbenzene moiety provided additional stability to **1**. Moreover, the TD-DFT calculated spectrum showed an absorption band at 343 nm (Fig. S3). This absorption band was due to a collection of electronic transitions from the HN_3O_2 ligand to Cu *d* orbitals. Therefore, we proposed that H-bonding at the oxygen atom of PhIO is more plausible structure.

3.3. Electron transfer reactivity of 1

The reactivity of the copper(II)-iodosylbenzene adduct, **1**, was first investigated in the electron transfer (ET) at 293 K. To examine the redox properties of **1**, the cyclic voltammetry was conducted in CH_3CN at 293 K. Electrochemical measurements of **1** were carried out in the −600 mV to +1500 mV range under aerobic conditions at different scan rates (Fig. 3a). While $[Cu(HN_3O_2)(CH_3CN)(H_2O)]^{2+}$ exhibited a nearly reversible $Cu^{II/I}$ couple with the redox potential (E_{red}) value of 0.08 V (vs SCE) [70], the irreversible oxidation (E_{pa}) and reduction (E_{pc}) peak potential values at 1.35 V (vs Ag/Ag^+) and −0.28 V (vs Ag/Ag^+), respectively, indicated the low thermodynamic stability of **1** during redox processes. Typically, the $E_{1/2}$ value of irreversible redox processes was found in the middle of E_{pa} and E_{pc} values. To estimate the $E_{1/2}$ value of **1**, the ET reaction between **1** and ferrocene (Fc) derivatives was explored. Upon addition of ferrocene (E_{ox} = 0.66 V vs Ag/Ag^+) into a CH_3CN-solution of **1**, the ET from Fc to **1** was monitored by an increase of the absorption band at 620 nm (ε = 400 cm^{-1} M^{-1}) due to the formation of ferrocenium ion (Fig. 3b). The pseudo-first order rate constant (k_{obs}) increased proportionally with an increasing concentration of Fc. The second-order rate constant (k_{et}) value (e.g., 1.3 × 10^{-2} M^{-1} s^{-1}) of ET from Fc to **1** was determined from the plot of the k_{obs} values against concentration of Fc (Fig. 3c). In parallel, the k_{et} value of ET from 1,1′-dimethylferrocene (E_{ox} = 0.55 V vs Ag/Ag^+) to **1** was determined to be 6.6 × 10^{-2} M^{-1} s^{-1} under identical reaction conditions (Fig. S4). However, **1** barely reacted with bromoferrocene (E_{ox} = 0.83 V vs Ag/Ag^+) under identical reaction conditions, indicating that the $E_{1/2}$ value of **1** might be positioned between 0.66 V (vs Ag/Ag^+) and 0.83 V (vs Ag/Ag^+).

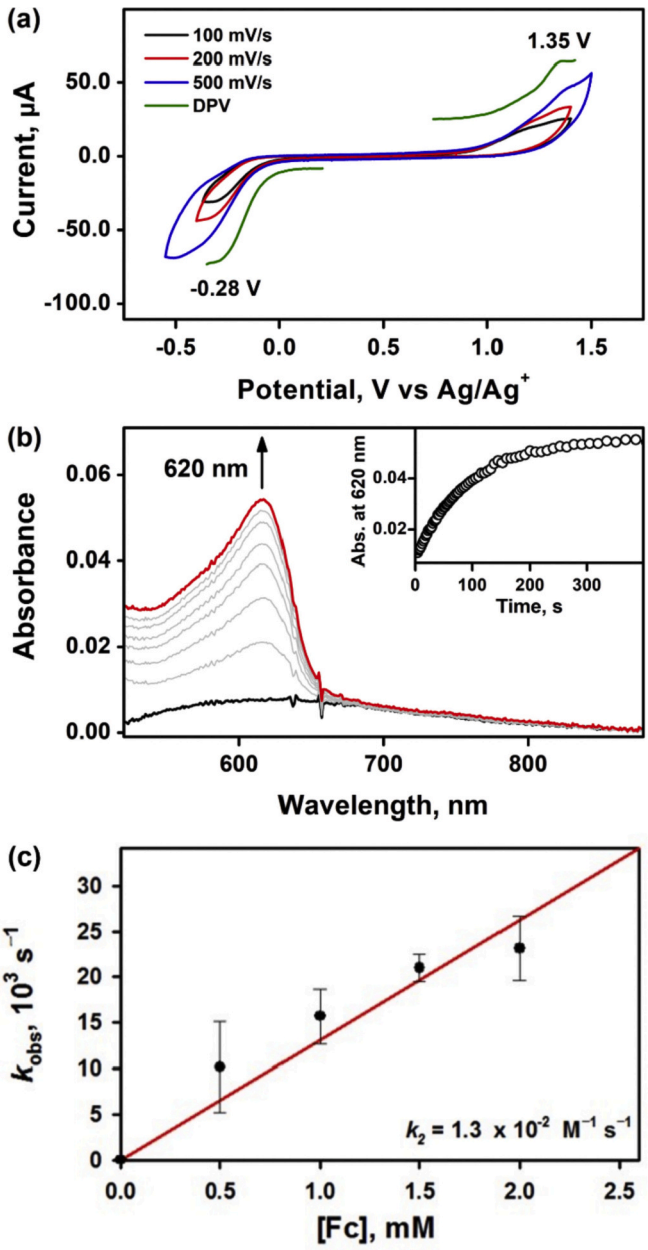

Fig. 3. (a) Cyclic voltammogram of **1** (2.0 mM) in CH_3CN containing $TBAPF_6$ (0.10 M) with a glassy carbon working electrode at various scan rates at 293 K. (b) UV–vis spectral changes observed in the ET reaction from Fc (0.50 mM) to **1** (0.10 mM) in CH_3CN at 293 K. (c) Plot of pseudo-first-order rate constants (k_{obs}) against the concentrations of Fc in CH_3CN at 293 K.

3.4. Catalytic reactivity of 1

With the metastable copper(II)-iodosylbenzene adduct, **1** in hand, the catalytic reactivity studies of **1** with substrates including thioanisole, cyclohexene, and styrene were carried out using PhIO as an oxidant. The oxygen atom transfer reaction was performed by adding **1** (0.10 mM) to a CH_3CN solution of thioanisole (100 mM) containing PhIO (10 mM) at 293 K under inert atmosphere (Fig. 4). The reactivity of **1** was expected to be low due to the H-bonding interaction between HN_3O_2 ligand and PhIO moiety. The catalytic reaction was carried over several hours. At the initial stage of the reaction, the methyl phenyl sulfoxide (i.e., two electron oxidized product) was obtained as the sole product with a

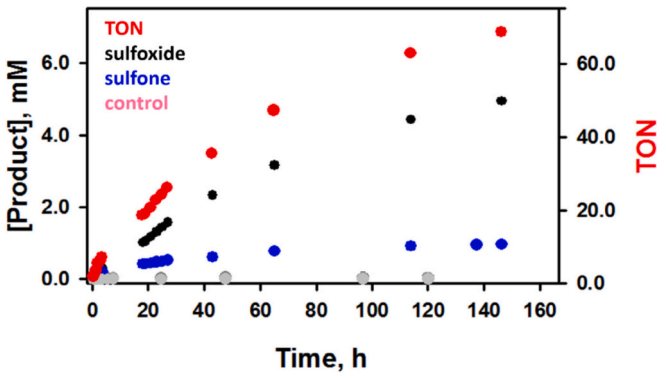

Fig. 4. Plot of concentrations of methyl phenyl sulfoxide (black dot), methyl phenyl sulfone (blue dot) and turnover number (red dot) obtained in the catalytic oxygen atom transfer reaction of thioanisole (100 mM) by $[Cu^{II}(HN_3O_2)(CH_3CN)(H_2O)](ClO_4)_2$ (0.10 mM) in the presence of PhIO (10 mM). Control experiments show that only trace amount of products (gray dot) were detected. (For interpretation of the references to colour in this figure legend, the reader is referred to the web version of this article.)

turnover number (TON) below 5 (i.e., 5% conversion yield; the TON and product yield were calculated on the basis of the concentration of PhIO). Interestingly, when the catalytic reaction proceeded over a day, the formation of methyl phenyl sulfone (i.e., four electron oxidized product) was detected. This evidently illustrated further oxidation of methyl phenyl sulfoxide. The maximum TON of sulfoxidation reached over 75 (i.e., 75% conversion yield). As the amount of products increased linearly and slowly over several hours, the initial reaction rate of the reaction was determined from the slope of the concentration of products against the reaction time. The formation rate of methyl phenyl sulfoxide and methyl phenyl sulfone were calculated to be 1.3×10^{-4} M h^{-1} and 2.4×10^{-5} M h^{-1}, respectively. Control experiment was also carried out under identical reaction conditions in the absence of copper(II) complex and the negligible amount (less than 0.1% conversion yield based on PhIO) was found (Fig. 4).

Recently, accumulated reports have demonstrated that mechanistically, there are two different reaction pathways for the sulfoxidation of thioanisole such as the direct oxygen atom transfer and electron transfer pathway; the latter pathway could be accelerated in the presence of acids. To evaluate the effect of acid on the catalytic activity of **1**, the catalytic sulfoxidation reactions were carried out in the presence of H_2SO_4. It is noteworthy that while the TONs of the catalytic reactions were similar, the initial reaction rates were clearly increased; 4.0×10^{-4} M h^{-1} in the presence of 10 equiv. of H_2SO_4 and 2.0×10^{-4} M h^{-1} in the presence of 5.0 equiv. of H_2SO_4 (Fig. S5). Additionally, other oxidants such as *tert*-butylhydroperoxide, and hydrogen peroxide were used under identical conditions, however, no formation of oxidized product was confirmed (Fig. S6). Thus, the reactive oxidant in the sulfoxidation reaction was the copper(II)-iodosylbenzene adduct (Scheme 2).

On the other hand, the oxidation of cyclohexene and styrene were carried out in order to examine the catalytic activity of **1** in the C—H bond activation and olefin epoxidation reactions. For instance, the oxidation of cyclohexene by **1** resulted in the formation of cyclohexenol, cyclohexenone, and cyclohexene oxide (Fig. S7). However, control experiment produced identical products with similar composition and yield, which led us to conclude that the catalytic oxidation of cyclohexene did not involve **1** but only PhIO, which was acting as sole reactive oxidant [71]. In case of styrene oxidation, the low catalytic activity of **1** did barely produce styrene oxide over the course of time (Fig. S8). For both cases, the presence of acids did not accelerate the reaction rates nor increase the product yields. This result was contradictory to that observed in the case of iodosylbenzene adduct of manganese, iron and cobalt complexes [36–38,41]. Plausible explanation of

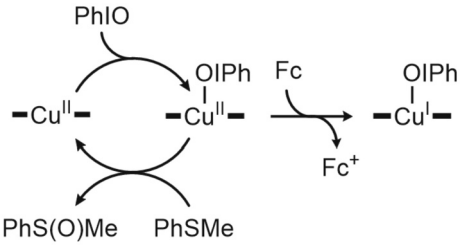

Scheme 2. The outlook of reactivity studies for **1** in the electron transfer and catalytic sulfoxidation reactions.

such low catalytic reactivity towards epoxidation and C—H bond activation reactions would be attributed to the intramolecular H-bonding interaction, which created additional steric hindrance for substrates to be in close interaction with iodosylbenzene moiety.

4. Conclusion

In summary, we have newly synthesized and characterized an iodosylbenzene adduct of a mononuclear copper(II) complex supported by a picolylamine based ligand with ethoxyethanol chain that created the intramolecular H-bonding interaction between HN_3O_2 ligand and iodosylbenzene moiety. DFT calculation suggested that the copper(II)-iodosylbenzene adduct having the intramolecular H-bonding interaction was energetically more favorable. The electron transfer reactivity of the copper(II)-iodosylbenzene adduct along with electrochemical measurement suggested that its redox potential was in the range of 0.66 V and 0.83 V (vs Ag/Ag^+). The present system displayed catalytic reactivity towards sulfoxidation reaction in the presence and absence of acid; the addition of acid accelerated the catalytic sulfoxidation presumably due to the enhancement of electron transfer rates. However, the epoxidation of styrene and the C—H bond activation of cyclohexene did not meet our expectation; the intramolecular H-bonding interaction might cause strong steric hindrance and inhibit the catalytic reactivity of the copper(II)-iodosylbenzene adduct. Further studies will be focused on the cleavage of the I—O bond processes in order to provide possible insight into the involvement of high-valent copper complexes.

Author contributions

S.H. conceived, designed the research and wrote the manuscript. H.J. and H.O. synthesized, run and analyzed the experimental and computational data. S.H. and H.J. discussed the results and contributed to the scientific interpretation.

Declaration of Competing Interest

The authors have no competing interests to declare.

Acknowledgments

This research was supported by the National Research Foundation of Korea (NRF), funded by the Korean government (NRF-2020R1C1C1008886 to S.H.)

Appendix A. Supplementary data

Supplementary data to this article can be found online at https://doi.org/10.1016/j.jinorgbio.2021.111524.

References

[1] J.M. Bollinger Jr., C. Krebs, Curr. Opin. Chem. Biol. 11 (11) (2007) 151–158.
[2] N. Fujieda, S. Yabuta, T. Ikeda, T. Oyama, N. Muraki, G. Kurisu, S. Itoh, J. Biol. Chem. 288 (2013) 22128–22140.

[3] G.R. Hemsworth, B. Henrissat, G.J. Davies, P.H. Walton, Nat. Chem. Biol. 10 (2013) 122–126.
[4] C.H. Kjaergaard, M.F. Qayyum, S.D. Wong, F. Xu, G.R. Hemsworth, D.J. Walton, N. A. Young, G.J. Davies, P.H. Walton, K.S. Johansen, K.O. Hodgson, B. Hedman, E. I. Solomon, Proc. Natl. Acad. Sci. U. S. A. 111 (2014) 8797–8802.
[5] T.V. Vendelboe, P. Harris, Y. Zhao, T.S. Walter, K. Harlos, K. El Omari, H.E. M. Christensen, Sci. Adv. 2 (2016) 1–10.
[6] D.A. Quist, D.E. Diaz, J.J. Liu, K.D. Karlin, J. Biol. Inorg. Chem. 22 (2017) 253–288.
[7] N. Mano, A. de Poulpiquet, Chem. Rev. 118 (2018) 2392–2468.
[8] S.M. Adam, G.B. Wijeratne, P.R. Rogler, D.E. Diaz, D.A. Quist, J.J. Liu, K.D. Karlin, Chem. Rev. 118 (2018) 10840–11022.
[9] X. Huang, J.T. Groves, Chem. Rev. 118 (2018) 2491–2553.
[10] N. Fujieda, K. Umakoshi, Y. Ochi, Y. Nishikawa, S. Yanagisawa, M. Kubo, G. Kurisu, S. Itoh, Angew. Chem. 132 (2020) 13487–13492.
[11] E.I. Solomon, D.E. Heppner, E.M. Johnston, J.W. Ginsbach, J. Cirera, M. Qayyum, M.T. Kieber-Emmons, C.H. Kjaergaard, R.G. Hadt, L. Tian, Chem. Rev. 114 (2014) 3659–3853.
[12] J.Y. Lee, K.D. Karlin, Curr. Opin. Chem. Biol. 25 (2015) 184–193.
[13] S. Itoh, Acc. Chem. Res. 48 (2015) 2066–2074.
[14] S. Hong, Y.-M. Lee, K. Ray, W. Nam, Coord. Chem. Rev. 334 (2017) 25–42.
[15] C.E. Elwell, N.L. Gagnon, B.D. Neisen, D. Dhar, A.D. Spaeth, G.M. Yee, W. B. Tolman, Chem. Rev. 117 (2017) 2059–2107.
[16] V.V. Vu, S.T. Ngo, Coord. Chem. Rev. 368 (2018) 134–157.
[17] S.M. Huber, M.Z. Ertem, F. Aquilante, L. Gagliardi, W.B. Tolman, C.J. Cramer, Chem. Eur. J. 15 (2009) 4886–4895.
[18] S. Kim, J. Ståhlberg, M. Sandgren, R.S. Paton, G.T. Beckham, Proc. Natl. Acad. Sci. U. S. A. 111 (2014) 149–154.
[19] G. Yassaghi, E. Andris, J. Roithová, Chem. Phys. Chem. 18 (2017) 2217–2224.
[20] E. Andris, R. Navrátil, J. Jašík, M. Puri, M. Costas, L. Que Jr., J. Roithoá, Angew. Chem. 131 (2019) 9721–9726.
[21] E. Andris, R. Navrátil, J. Jašík, M. Srnec, M. Rodríguez, M. Costas, J. Roithoá, Angew. Chem. 131 (2019) 9721–9726.
[22] V.A. Larson, B. Battistella, K. Ray, N. Lehnert, W. Nam, Nat. Rev. Chem. 4 (2020) 404–419.
[23] J. Sun, D. Zhang-Negrerie, Y. Du, K. Zhao, Rep. Org. Chem. 6 (2016) 25–45.
[24] A. Gunay, K.H. Theopold, Chem. Rev. 110 (2010) 1060–1081.
[25] Z. Chen, G. Yin, Chem. Soc. Rev. 44 (2015) 1083–1100.
[26] X. Engelmann, I. Monte-Pérez, K. Ray, Angew. Chem. Int. Ed. 55 (2016) 7632–7649.
[27] S.C. Hammer, G. Kubik, E. Watkins, S. Huang, H. Minges, F.H. Arnold, Science 358 (2017) 215–218.
[28] S. Fukuzumi, T. Kojima, Y.-M. Lee, W. Nam, Coord. Chem. Rev. 333 (2017) 44–56.
[29] M. Guo, T. Corona, K. Ray, W. Nam, ACS Cent. Sci. 5 (2019) 13–28.
[30] S. Fukuzumi, K.-B. Cho, Y.-M. Lee, S. Hong, W. Nam, Chem. Soc. Rev. 49 (2020) 8988–9027.
[31] M. Guo, Y.-M. Lee, S. Fukuzumi, W. Nam, Coord. Chem. Rev. 435 (2021) 213807.
[32] W. Nam, S.K. Choi, M.H. Lim, J.-U. Rohde, I. Kim, J. Kim, C. Kim, L. Que Jr., Angew. Chem. Int. Ed. 42 (2003) 109–111.
[33] C. Wang, T. Kurahashi, H. Fujii, Angew. Chem. 124 (2012) 7929–7931.
[34] A. Lennartson, C.J. McKenzie, Angew. Chem. 124 (2012) 6871–6874.
[35] M. Guo, H. Dong, J. Li, B. Cheng, Y.-q. Huang, Y.-q. Feng, A. Lei, Nat. Commun. 3 (2012) 1190.
[36] S. Hong, B. Wang, M.S. Seo, Y.-M. Lee, M.J. Kim, H.R. Kim, T. Ogura, R. Garcia-Serres, M. Clémancey, J.-M. Latour, W. Nam, Angew. Chem. Int. Ed. 53 (2014) 6388–6392.
[37] M. Guo, Y.-M. Lee, M.S. Seo, Y.-J. Kwon, X.-X. Li, T. Ohta, W.-S. Kim, R. Sarangi, S. Fukuzumi, W. Nam, Inorg. Chem. 57 (2018) 10232–10240.
[38] D. Jeong, T. Ohta, J. Cho, J. Am. Chem. Soc. 140 (2018) 16037–16041.
[39] J.R. Winkler, H.B. Gray, D. Mingos, P. Day, J. Dahl (Eds.), Molecular Electronic Structures of Transition Metal Complexes I. Structure and Bonding, Springer, Berlin, Heidelberg, 2011.
[40] E.A. Hill, M.L. Kelty, A.S. Filatov, J.S. Anderson, Chem. Sci. 9 (2018) 4493–4499.
[41] J. Yang, M.S. Seo, K.H. Kim, Y.-M. Lee, S. Fukuzumi, J. Shearer, W. Nam, Angew. Chem. Int. Ed. 59 (2020) 13581–13585.
[42] W.L.F. Armarego, C.L.L. Chai, Purification of Laboratory Chemicals, 6th ed., Pergamon Press, Oxford, 2009.
[43] H. Oh, W.-M. Ching, J. Kim, W.-Z. Lee, S. Hong, Inorg. Chem. 58 (2019) 12964–12974.
[44] M.J. Frisch, G.W. Trucks, H.B. Schlegel, G.E. Scuseria, M.A. Robb, J.R. Cheeseman, G. Scalmani, V. Barone, G.A. Petersson, H. Nakatsuji, X. Li, M. Caricato, A. Marenich, J. Bloino, B.G. Janesko, R. Gomperts, B. Mennucci, H.P. Hratchian, J. V. Ortiz, A.F. Izmaylov, J.L. Sonnenberg, D. Williams-Young, F. Ding, F. Lipparini, F. Egidi, J. Goings, B. Peng, A. Petrone, T. Henderson, D. Ranasinghe, V. G. Zakrzewski, J. Gao, N. Rega, G. Zheng, W. Liang, M. Hada, M. Ehara, K. Toyota, R. Fukuda, J. Hasegawa, M. Ishida, T. Nakajima, Y. Honda, O. Kitao, H. Nakai, T. Vreven, K. Throssell, J.A. Montgomery Jr., J.E. Peralta, F. Ogliaro, M. Bearpark, J.J. Heyd, E. Brothers, K.N. Kudin, V.N. Staroverov, T. Keith, R. Kobayashi, J. Normand, K. Raghavachari, A. Rendell, J.C. Burant, S.S. Iyengar, J. Tomasi, M. Cossi, J.M. Millam, M. Klene, C. Adamo, R. Cammi, J.W. Ochterski, R.L. Martin, K. Morokuma, O. Farkas, J.B. Foresman, D.J. Fox, Gaussian 09, Revision A.02, Gaussian, Inc., Wallingford CT, 2016.
[45] T.H. Dunning Jr., P.J. Hay, in: H.F. Schaefer III (Ed.), Modern Theoretical Chemistry, Plenum, New York, 1977.
[46] P.J. Hay, W.R. Wadt, J. Chem. Phys. 82 (1985) 270–283.
[47] W.R. Wadt, P.J. Hay, J. Chem. Phys. 82 (1985) 284–298.
[48] P.J. Hay, W.R. Wadt, J. Chem. Phys. 82 (1985) 299–310.
[49] R. Ditchfield, W.J. Hehre, J.A. Pople, J. Chem. Phys. 54 (1971) 724–728.
[50] W.J. Hehre, R. Ditchfield, J.A. Pople, J. Chem. Phys. 56 (1972) 2257–2261.
[51] P.C. Hariharan, J.A. Pople, Theor. Chem. Accounts 28 (1973) 213–222.
[52] P.C. Hariharan, J.A. Pople, Mol. Phys. 27 (1974) 209–214.
[53] M.S. Gordon, Chem. Phys. Lett. 76 (1980) 163–168.
[54] M.M. Francl, W.J. Pietro, W.J. Hehre, J.S. Binkley, D.J. DeFrees, J.A. Pople, M. S. Gordon, J. Chem. Phys. 77 (1982) 3654–3665.
[55] R.C. Binning Jr., L.A. Curtiss, J. Comp. Chem. 11 (1990) 1206–1216.
[56] J.-P. Blaudeau, M.P. McGrath, L.A. Curtiss, L. Radom, J. Chem. Phys. 107 (1997) 5016–5021.
[57] V.A. Rassolov, J.A. Pople, M.A. Ratner, T.L. Windus, J. Chem. Phys. 109 (1998) 1223–1229.
[58] V.A. Rassolov, M.A. Ratner, J.A. Pople, P.C. Redfern, L.A. Curtiss, J. Comp. Chem. 22 (2001) 976–984.
[59] M. Cossi, N. Rega, G. Scalmani, V. Barone, J. Comput. Chem. 24 (2003) 669–681.
[60] A.D. McLean, G.S. Chandler, J. Chem. Phys. 72 (1980) 5639–5648.
[61] K. Raghavachari, J.S. Binkley, R. Seeger, J.A. Pople, J. Chem. Phys. 72 (1980) 650–654.
[62] J.-P. Blaudeau, M.P. McGrath, L.A. Curtiss, L. Radom, J. Chem. Phys. 107 (1997) 5016–5021.
[63] A.J.H. Wachters, J. Chem. Phys. 52 (1970) 1033–1036.
[64] P.J. Hay, J. Chem. Phys. 66 (1977) 4377–4384.
[65] K. Raghavachari, G.W. Trucks, J. Chem. Phys. 91 (1989) 1062–1065.
[66] R.C. Binning Jr., L.A. Curtiss, J. Comp. Chem. 11 (1990) 1206–1216.
[67] M.P. McGrath, L. Radom, J. Chem. Phys. 94 (1991) 511–516.
[68] L.A. Curtiss, M.P. McGrath, J.-P. Blaudeau, N.E. Davis, R.C. Binning Jr., L. Radom, J. Chem. Phys. 103 (1995) 6104–6113.
[69] T. Clark, J. Chandrasekhar, G.W. Spitznagel, P.V.R. Schleyer, J. Comp. Chem. 4 (1983) 294–301.
[70] H. Oh, S. Choi, J.Y. Kim, H.S. Ahn, S. Hong, Chem. Commun. 55 (2019) 12659–12662.
[71] S.J. Kim, R. Latifi, H.Y. Kang, W. Nam, S.P. de Visser, Chem. Commun. (2009) 1562–1564.